

AUTOMATED OBJECT-BASED IDENTIFICATION OF DUNES AT HARGRAVES CRATER, MARS. A. Emran¹, L. J. Marzen¹, and D. T. King Jr.¹, ¹Department of Geosciences, Auburn University, 2050 Beard Eaves Coliseum, Auburn, AL 36849. (aze0024@auburn.edu).

Introduction: Terrestrial dune fields are good indicator of past and present aeolian transport regimes of planets like Earth, Mars, and Venus [e.g., 1; and references therein]. Aeolian processes provide insight into the interactions between the atmosphere and the surface of Mars as well as the weather, climate, and climatic evolution along the Martian history [2-3].

A complete catalogue for Martian dune fields, leveled as the Mars Global Digital Dune Database (MGD³), contains information about locations and characteristics of dune fields as well as other parameters [4-5]. The MGD³, done by manual visual photo interpretation from the Thermal Emission Imaging System [THEMIS; 6] of 100 m/pixel images, needs to be updated for a better understanding of surface and atmospheric mechanisms of Mars. This study used an automated object-based image analysis (OBIA) technique from the Context Camera [CTX; 7] image of ~6 m/pixel dataset to extract more quick, reliable, and accurate identification of the dunes at Hargraves crater, Mars. Having many advantages over the pixel-based photo interpretation, OBIA can produce more robust and accurate results in detecting dunes on Mars. The study, indeed, is a test case and if proven reliable then the method can be applied to the entire Martian surface to make a higher resolution dune database, which will be an updated version of existing database. The Hargraves crater is located on the Jezero crater watershed on Mars, centered on 75.75° E and 20.75° N (Fig.1).

Methods: CTX grayscale (back and white-panchromatic; PAN) image and its stereopair-derived digital elevation models (DEMs) were used as dataset layers for OBIA processing. The USGS's Integrated Software for Imagers and Spectrometers (ISIS3) pipelines and NASA Ames Stereo Pipeline (ASP) stereo-grammetry software [8-10] were used for the calibration, projection, and producing the DEMs from CTX stereopair. Our OBIA methodology consists of an application of image segmentation into a set of image objects whose parameters were then used to classify dunes from the non-dune object using eCognition software package. We used 'multi-resolution segmentation' algorithm where weights of the layers were given as 1:4 to DEM and PAN layers, respectively. The scale parameter was set as 40 whereas shape was fixed to 0.6 and compactness was set as 0.5. After the successful segmentation of image objects, a set of rulesets (e.g., object thresholding) were applied to the image objects

to differentiate dune from non-dune objects. The dune objects were then classified and exported into a vector file format including different geometric parameters (e.g., area, lengths, perimeter etc.). Lastly, we assessed the accuracy of the classified dune objects considering around 500 random points in the study area.

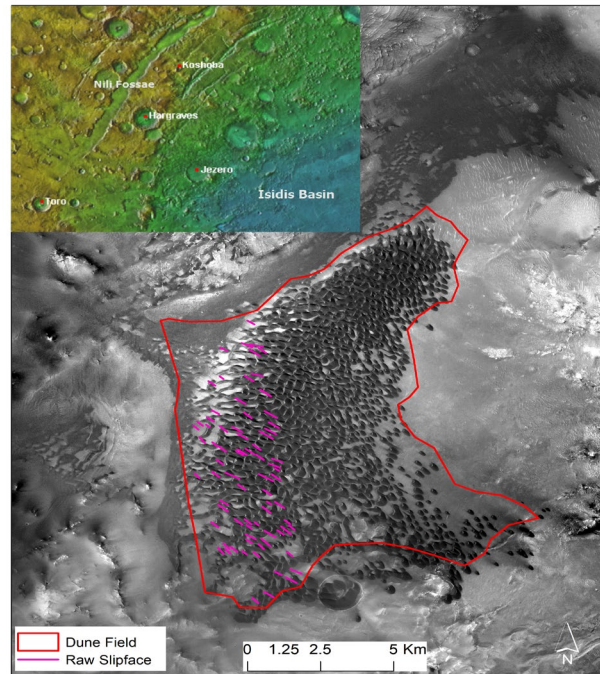


Fig 1: Dune distribution of Hargraves crater, inset is the location of study area. The dune fields and slipface outlined here are derived from the MGD³.

Results: We prepared a vector (ESRI .shp) file for the dunes at Hargraves crater. The dunes vector data were then analyzed qualitatively (e.g., visual interpretation) and quantitatively (e.g., accuracy assessment). The MGD³ maps dune fields at Hargraves as a whole (not appropriate though) but our dune database includes individual dunes and their geometric information (e.g., length, perimeter, area etc.). The results we presented here are the outcomes from our preliminary research. The MGD³ identified a total area of ~100 sq. km of dune field at Hargraves whereas this study found a total of ~70 sq. km of dune areas. This difference is because we only included dune areas excluding the outlined surrounding areas. Our result shows almost perfect match with the dune distribution as assessed through visual photo inspection (Fig. 2). The accuracy of the dune classification was conducted

through a quantitative assessment in this study. The projected CTX images were used as the reference dataset to evaluate the accuracy of the classified dunes.

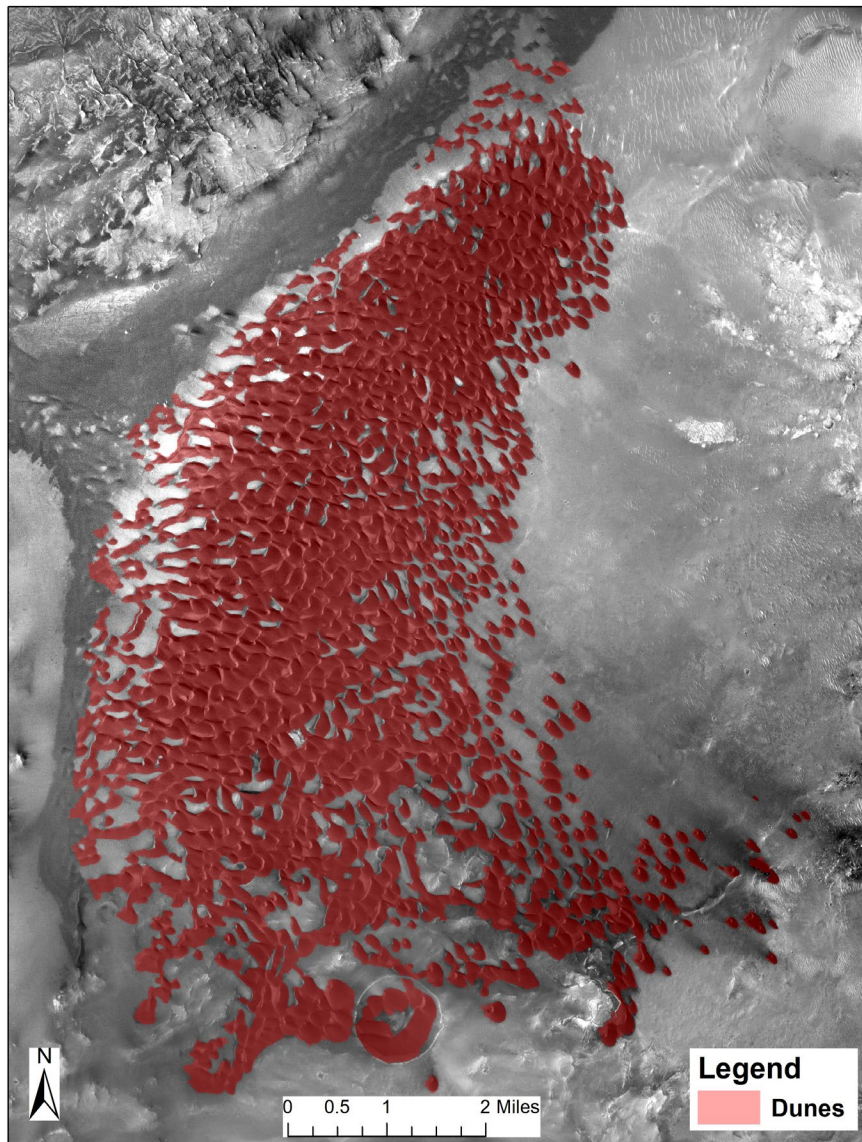


Fig. 2: Distribution of the classified dunes at Hargraves.

Table 1: Accuracy assessment result of the classification.

Accuracy	User (%)	Producer (%)
Dune	98.31	88.45
Non-dune	81.37	97.08
Overall (OA)	0.91 or 91%	
Kappa coefficient	0.82 or 82%	

We used error matrix to evaluate the accuracy of our classification through assessing overall accuracy (OA) and kappa coefficient (*kappa*) statistics. Typically, the higher OA and *kappa* value indicate the higher

level of accuracy of classification. We assessed the producer and user accuracy for the dune classification were 88% and 98%, respectively (Table 1). The overall accuracy and the kappa coefficient were 91% and 82%, respectively (Table 1). Having proved the higher accuracy and validated method we assert that OBIA technique can be applied to whole Martian surface for an updated dune database.

Conclusion: The delineation of dune fields in MGD³ were prepared manually through visual photo-interpretation from the THEMIS imagery at 100 m/pixel spatial resolution, including the digitized dune parameters and mapped dune slipface orientations. However, the manual digitizing of the dune parameters from low resolution THEMIS images demands very tedious and time-consuming task. Therefore, an automated method from high resolution images e.g., CTX at ~6 m/pixel are more efficient to maximize the extraction of valuable geomorphological information of Martian dune fields. We employed an automated object-based image analysis technique to extract dunes at Hargraves as a test case of OBIA application. Our validated and accurate result indicates the applicability of the OBIA method for the entire surface of Mars.

References: [1] Vaz D.A. et al. (2015) *Geomorphology*, 250, 128–139. [2] Greeley R. et al. (2001) *Space Science Reviews*, 96, 393–404. [3] Wilson S.A. and Zimbelman, J.R. (2004) *JGR*, 109, E10. [4] Hayward R.K. et al. (2014) *Icarus*, 230, 9. [5] Hayward R.K. et al. (2007) *JGR*, 112. [6] Christensen P.R. et al. (2004) *JGR*, 106, 23823–23871. [7] Malin M.C. (2007) *JGR*, 112, E05S04. [8] Broxton M.J. and Edwards, L.J. (2008) *LPS XXXIX*, Abstract# 2419. [9] Moratto Z.M. et al. (2010) *LPS XXXXI*, Abstract# 2364. [10] Beyer R.A. et al. (2014) *LPS XXXXV*, Abstract# 2902.